ELSEVIER

Journal of Hydrology 175 (1996) 511–532

Journal of Hydrology

Stochastic storm transposition coupled with rainfall–runoff modeling for estimation of exceedance probabilities of design floods

M. Franchini[a,*], K.R. Helmlinger[b,1], E. Foufoula-Georgiou[b], E. Todini[a]

[a]*Istituto di Costruzioni Idrauliche, Facoltà di Ingegneria, Viale Risorgimento 2, 40136 Bologna, Italy*

[b]*St. Anthony Falls Hydraulic Laboratory, University of Minnesota, Mississippi River at 3rd Avenue S.E., Minneapolis, MN 55414-2196, USA*

Received 2 March 1995; accepted 30 March 1995

Abstract

The stochastic storm transposition (SST) technique has been developed and evaluated in previous studies for the estimation of exceedance probabilities of extreme precipitation depths. In this study it is extended to the estimation of exceedance probabilities of extreme design floods. The link between storms and flood peaks is provided by a rainfall–runoff transformation and stochastic descriptions of antecedent moisture conditions and storm depth temporal distributions. Cumulative average catchment depths produced by the SST approach have been converted to a range of possible flood peak values using a rainfall–runoff model (the ARNO model) and a probabilistic disaggregation scheme of cumulative storm depths to hourly data. The analysis has been repeated for a range of fixed antecedent moisture conditions. The probabilities of exceedance of the produced flood peaks have been estimated and compared to highlight the effect of antecendent moisture conditions on the magnitude and frequency of produced floods as compared with the magnitude and frequency of the corresponding average catchment depths.

1. Introduction

It has been argued over the years that it is not feasible to estimate exceedance probabilities of very extreme floods or equivalently is not feasible to estimate the magnitude of very infrequent flood peaks, i.e., events of return period greater than 10^3–10^4 years. Thus for the design of very large hydraulic structures, where failure

* Corresponding author.

[1] Present address: Higher Dimension Research, Inc., St. Paul, MN, USA.

SSDI 0022-1694(95)02847-1

could cause possible loss of life and substantial property damage, deterministic (instead of risk-based) procedures have normally been used for estimation of the magnitude of design events. These estimates have mostly been based on the probable maximum flood (PMF) procedure, where probable maximum precipitation (PMP) estimates are deterministically converted to floods (e.g. see Wang and Jawed, 1986). PMF is defined as the flood resulting from the 'extreme application' over the basin of the PMP. PMP is the 'theoretically greatest depth of precipitation that is physically possible over a particular drainage area at a certain time of the year' (Huschke, 1959, p. 446). Although standardized methods of computing PMP and PMF estimates are usually used (e.g. see World Meterological Organization, 1973), the large subjectivity involved in the whole estimation process has several times led to estimation of significantly different values of design events by different agencies for the same location. A case in point is the Harriman dam in the upper Deerfield river basin (518 km^2, or 200 square miles) in Whitingham, Virginia, for which the 24 h 200 square miles PMP value was estimated by the Yankee Atomic Electric Company in 1980 as 363 mm (14.3 in), by the Franklin Research Institute in 1982 as 373 mm (14.7 in) and by the National Weather Service (NWS) in 1983 as more than 560 mm (22 in) (see Yankee Atomic Energy Company (YAEC), 1984). Another concern with the PMF estimates is that they might have different chances of being exceeded in different regions of the USA, which would mean an unequal level of flood protection at different sites. For example, Kraeger and Franz (1992) have estimated that the NWS PMF estimate for the Russian River, California, has a return period of more than 100 000 years, whereas that for the Sulphur River, Texas, has a return period of 4000–5000 years, and for the Atlamaha River, Georgia, has a return period of 2.5 billion years.

Motivated by these problems, Foufoula-Georgiou (1989) and Wilson and Foufoula-Georgiou (1990) developed a stochastic storm transposition (SST) approach, which emulates in a probabilistic framework the PMP estimation process, as a possible method of assessing the exceedance probability of very extreme precipitation depths. The underlying idea of the SST approach is the enlargement of the record of storms available for estimation by considering storms that have not occurred over the catchment of interest but that could have occurred over it. This approach leads to storm regionalization and estimation of the joint probability distribution of storm characteristics and storm occurrences within a prespecified storm transposition area. To date, the SST approach has been applied only for the estimation of exceedance probabilities of areally averaged catchment depths. What is needed for design, however, is flood peaks and volumes. In this paper, the SST technique has been extended to a probabilistic procedure for estimation of annual exceedance probabilities of flood peaks and volumes by coupling it with a rainfall–runoff model.

Many rainfall–runoff models are available, ranging from very simple lumped schemes (e.g. the curve number method) to very complicated, differential, distributed models (e.g. the SHE model, Abbott et al., 1986). In selecting a rainfall–runoff model to be used in a combined storm–runoff statistical analysis one has to define the aspects that are considered of primary importance in the physical rainfall–runoff transformation process. It is well recognized that the water storage capacity of the

soil and its initial water content are the most important aspects that affect the peak-runoff production process. Drainage and translation along hillslopes and network channels have a minor influence on the peak runoff production even if they maintain a significant influence on the flood volumes. In other words, the most important aspect to be well represented is the water balance component at soil level. This consideration allows us to avoid using extremely complicated models such as SHE, where, in addition, the large number of physical parameters to be defined at grid level would produce high uncertainty and render the Monte Carlo process totally impractical. On the other hand, extremely simplified models seem not to be sufficiently accurate to perform a reliable analysis. Thus the range of candidate models can be restricted to only a few conceptual ones.

Recently, Franchini and Pacciani (1991) have carried out a comparative analysis of several rainfall–runoff conceptual models (STANFORD, SACRAMENTO, TANK, ARNO, etc.) and have shown that significantly different models produce basically equivalent results, although the difficulty in understanding the sensitivity of the results to the model parameters increases in proportion to the complexity of the model structure. According to these results, the ARNO model has been considered as one of the most appropriate models to perform flood peak frequency analysis. In fact, it balances well a relatively complex structure with a probabilistic description of the spatial distribution of water storage capacity.

This paper is arranged as follows. In the next section a brief description of the SST approach and the ARNO model is given, and the technique of coupling the SST approach with a rainfall–runoff model for estimation of exceedance probabilities of extreme flood peaks is developed. Then, we describe the set of available extreme storm data used in the analysis together with the distributional assumptions in the stochastic description of storm and basin characteristics. In Section 4 we present the results of an application of the flood peak frequency analysis method to a real case study, discuss the possible use of the obtained estimates in hydraulic design decisions, and illustrate the sensitivity of the results to antecedent moisture conditions of the basin. The paper ends with some concluding remarks on the still controversial subject of extreme flood frequency analysis and its use in design.

2. Methods

2.1. Brief description of the SST approach

Let $d(x, y, t)$ denote the rainfall depth deposited from a storm at the ground location of spatial coordinates (x, y) during a period of time $(0, t]$. For design purposes, a variable of particular interest is the maximum areally averaged depth that can occur over a catchment of area A_c during a time period Δt, i.e.

$$\overline{d_c}(\Delta t) = \frac{1}{|A_c|} \iint_{A_c} [d(x, y, t_s + \Delta t) - d(x, y, t_s)] \, dx \, dy \tag{1}$$

where the period Δt is equal to a critical duration of rainfall in terms of flood production, and t_s is defined such that

$$\iint_{A_c} [d(x,y,t_s+\Delta t) - d(x,y,t_s)]\,\mathrm{d}x\,\mathrm{d}y \geq$$

$$\times \iint_{A_c} [\mathrm{d}(x,y,t+\Delta t) - d(x,y,t)]\,\mathrm{d}x\,\mathrm{d}y \quad \forall \quad t < t_r - \Delta t \tag{2}$$

where t_r is the storm duration.

Let $\mathbf{\Lambda}_s$ denote the random vector of storm characteristics describing a storm. In general, $\mathbf{\Lambda}_s$ will be composed if the parameters of a stochastic model describing the rainfall field. Depending on the model, these parameters may or may not be directly interpretable in terms of physical storm characteristics. Let $\mathbf{\Lambda}_p$ denote the two-dimensional vector describing the position of a storm (here this position is called the storm center). The storm center may be defined as the location of the maximum observed total depth or as the location of the maximum accumulated depth over a specified period of time. Alternatively, it may be defined as the center of mass of the storm. Denoting by $\mathbf{\Omega} = (\mathbf{\Lambda}_s, \mathbf{\Lambda}_p)$ the joint vector of storm characteristics and storm positions, the cumulative distribution function of $\overline{d_c}(\Delta t)$ can be expressed as

$$F(d) \equiv F_{\overline{d_c}(\Delta t)}(d) = \mathrm{pr}(\overline{d_c}(\Delta t) \leq d) = \int_{\mathbf{\Omega}} \mathrm{pr}(\overline{d_c}(\Delta t) \leq d\,|\omega)\,\mathrm{d}\,F_{\mathbf{\Omega}}(\omega) \tag{3}$$

where $F_{\mathbf{\Omega}}(\omega)$ is the cumulative joint distribution function of the random vector $\mathbf{\Omega}$. Of interest is the exceedance probability of $\overline{d_c}(\Delta t)$, which can be obtained as

$$G(d) \equiv G_{\overline{d_c}(\Delta t)}(d) = 1 - F(d) \tag{4}$$

Let $Z(t)$ denote the counting process of the number of extreme storms in an interval of t years (stationarity in time is assumed). The annual exceedance probability can be expressed as

$$G^a(d) = 1 - \sum_{\nu=0}^{\infty} \mathrm{pr}[\overline{d_c}(\Delta t) \leq d\,|Z(1) = \nu] \cdot \mathrm{pr}[Z(1) = \nu] \tag{5}$$

Assuming that $Z(1)$, the random variable of the number of extreme storm occurrences per year, is independent of the storm depths $\overline{d_c}(\Delta t)$, and that $\overline{d_c}(\Delta t)$ are independent and identically distributed random variables, the annual probability of exceedance of $\overline{d_c}(\Delta t)$ can be written as

$$G^a(d) = 1 - \sum_{\nu=0}^{\infty} [F_{\overline{d_c}(\Delta t)}(d)]^{\nu} \cdot \mathrm{pr}[Z(1) = \nu] \tag{6}$$

Assuming that $Z(1)$ follows a Poisson distribution with annual occurrence rate λ (this is a realistic assumption shown by Wilson and Foufoula-Georgiou (1990) to hold true for the midwestern extreme storms considered in this study), the annual exceedance

probability of $\overline{d_c}(\Delta t)$ can be shown to be

$$G^a(d) = 1 - \exp[-\lambda G(d)] \tag{7}$$

Throughout the rest of the paper, $F_{\overline{d_c}(\Delta t)}(d)$ will be abbreviated as $F(d)$ and $F^a_{\overline{d_c}(\Delta t)}(d)$ ad $F^a(d)$. $G(d)$ and $G^a(d)$ represent similar abbreviations.

2.2. ARNO model

Two distinct components may be identified in the ARNO model (Todini, 1996). The first represents the soil-level water balance and the second the transfer to the outlet of the basin. The part representing the soil-level water balance is the most important and characterizes the model. It expresses the balance between the moisture content of the soil and the incoming (precipitation) and outgoing (evapotranspiration and runoff) quantities. The runoff is then subjected to a transfer operation which represents (1) the transfer to the network channels along the hillslopes, and (2) the transfer to the outlet of the basin along the channel network. The reader should refer to Todini (1996) for a more detailed description of the ARNO model.

2.3. Stochastic storm transposition coupled with rainfall–runoff modeling

Stochastic storm transposition (SST) is an event-type approach which provides values (and their associated exceedance probabilities) of cumulative precipitation depths over a specified period of time and averaged over the catchment area. Thus, in coupling SST with a rainfall–runoff (R–R) model, it is not possible to perform a continuous simulation with the R–R model but only event simulation. In this case, specification of the initial moisture condition plays an important role in the obtained distribution of flood peaks. Let us assume that the initial moisture condition, specified in the ARNO model with the parameter W_0, is a random variable with a probability distribution $F_{W_0}(w_0)$. This probability distribution must be estimated from antecedent moisture conditions of extreme storm events.

To obtain runoff hydrographs the cumulative precipitation depths provided by the SST approach have to be distributed in small time intervals (e.g. hours) over their durations, as required by the time step of the R–R model. Let $T(t)$ denote the set of nondimensional curves (mass curves) describing all possible temporal distributions of the cumulative precipitation depth over a specified duration and $f_{T(t)}(\tau(t))$ its probability distribution. As it is well known that the temporal distribution of extreme storm depths considerably affects the magnitude of the produced flood peaks, it is important to have a good estimate of the probability distribution of $\tau(t)$. For this estimation hourly rainfall data from several extreme storms are needed.

Finally, the basin characteristics, indirectly expressed by the parameters of the R–R model, also play an important role in the produced runoff peaks and volumes. Let us denote by Ψ the vector of these parameters and by $f_\Psi(\psi)$ the joint probability distribution of this vector. Most of the parameters of Ψ represent physical characteristics of the basin and may thus be considered as deterministic quantities to be estimated from calibration of the R–R model.

To obtain the probability of exceedance of flood peaks integration must be performed now not only over the random storm characteristics and locations (random vector $\mathbf{\Omega}$) but also over the random quantities W_0, Ψ, and $T(t)$. Assuming that basin characteristics, initial soil moisture, and temporal distributions of storms are independent of each other, the exceedance probability of the peak runoff Q_p can be written as

$$G(q) = 1 - \int_{\Omega}\int_{W_0}\int_{\Psi}\int_{T(t)} \mathrm{pr}\,[Q_p \le q|\omega, w_0, \psi, \tau(t)] \times f_{\Omega}(\omega) f_{W_0}(w_0,) f_{\Psi}(\psi) f_{T(t)}(\tau(t))\,\mathrm{d}\omega\,\mathrm{d}\omega_0\,\mathrm{d}\psi\,\mathrm{d}\tau(t) \tag{8}$$

Finally, assuming that the number of extreme flood peaks per year follows a Poisson distribution with annual occurrence rate λ', the annual exceedance probability of flood peaks is given as

$$G^a(q) = 1 - \exp\,[-\lambda' G(q)] \tag{9}$$

3. Area of application and distributional assumptions

3.1. Storm characteristics

The area of study is the nine-state midwestern area of North Dakota, South Dakota, Nebraska, Kansas, Minnesota, Iowa, Missouri, Wisconsin, and Illinois shown in Fig. 1. This area was selected for its homogeneous climatological conditions, lack of orography, and existence of data of very extreme precipitation events over a period of more than 100 years as reported in the US Army Corps of Engineers (1945–) storm catalog. All storms in the catalog which have their centers within this region and for which the maximum recorded 24 h average depth ($\Delta t = 24$ h) was greater than or equal to 20.32 cm (8.0 in) were used. Sixty-five such storms were identified, and a summary of their characteristics is given in Table 1. More details on these storms have been given by Wilson and Foufoula-Georgiou (1990). For each storm the maximum 24 h amount was used and was distributed in space according to a spread function fitted to the depth–area–duration (DAD) curves reported in the US Army Corps of Engineers catalog. This procedure produces maximum average depths over areas of given sizes, which is what is typically used for design.

It was assumed that the maximum 24 h depth distribution within the storm area enclosed by the contour of 7.62 cm (3 in) (this area is referred to here as the storm area A_s) is described by homocentric, geometrically similar contours around a single center. These contours were further approximated by ellipses of major to minor axis ratio equal to c and orientation of major axis equal to ϕ (this angle being measured counterclockwise from the horizontal east–west direction). To distribute spatially the maximum 24 h average depth over an area A, (e.g. $\bar{d}(A)$), the following

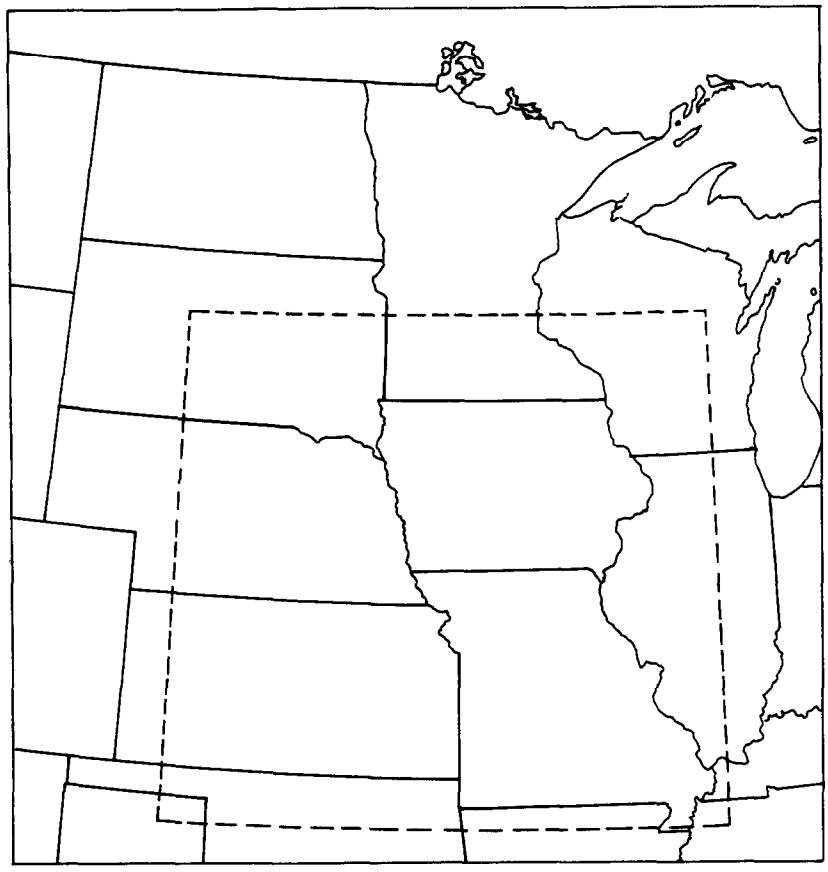

Fig. 1. The nine-state midwestern region and storm transposition area (dashed line) used in the analysis.

spread function was assumed:

$$\bar{d}(A) = d_o^* \exp(-kA^n) \tag{10}$$

where d_o^* represents the maximum 24 h recorded depth, taken as the storm center depth, and k and n are parameters estimated for each individual storm.

The above simplified description of the storm's spatial pattern results in the representation of the random vector $\boldsymbol{\Omega}$ by the following random variables

$$\boldsymbol{\Omega} = [D_o^* K^* N C \Phi X Y]' \tag{11}$$

where the prime denotes transpose, and D_o^*, K^*, N, C, and Φ denote the random variables taking on values d_o^*, k, n, c and ϕ, respectively, and (X, Y) denotes the random vector of the spatial coordinates of the storm center position.

From a statistical and cross-correlation analysis of the characteristics of the analyzed storms, Wilson and Foufoula-Georgiou (1990) reported the following

Table 1
Characteristics of the extreme midwestern storms used in the analysis

Storm no.	US Army Corps of Engineers	Duration (h)	Max 24 h depth (in)	Areal extent (square miles) (associated average depth (in))	Storm center		
					Town	State	Date
1	MR 4-24	54	24.0	63300 (2.7)	Boyden	IA	Sept. 1926
2	MR 4-5	20	13.0	20000 (3.5)	Grant Township	NE	June 1940
3	MR 6-15	78	15.8	16000 (2.9)	nr. Station	NE	June 1944
4	MR 7-2A	78	15.0	45000 (2.9)	nr. Cole Camp	MO	Aug. 1946
5	MR 1-10	96	14.7	59000 (2.9)	Woodburn	IA	Aug. 1903
6	MR 2-29	78	12.2	113500 (1.5)	Grant City	MO	July 1922
7	MR 1-5	78	12.3	100000 (2.0)	Primghar	IA	July 1900
8	MR 10-2	108	9.3	57000 (2.5)	Council Grove	KS	July 1951
9	MR 8-20	120	12.0	306000 (0.7)	nr. Holt	MO	June 1947
10	MR 1-9	168	8.1	136000 (1.2)	Abilene	KS	May 1903
11	MR 3-14	120	8.8	120000 (2.2)	Pleasanton	KS	Sept. 1927
12	MR 4-2	96	12.9	30000 (2.4)	Larrabee	IA	June 1891
13	UMV 1-11	108	11.5	50000 (2.0)	Ironwood	MI	July 1909
14	UMV 2-18	180	8.1	70000 (1.8)	Boonville	MO	Sept. 1905
15	UMV 1-22	78	12.4	60000 (2.2)	Haywood	WI	Aug. 1941
16	OR 4-8	90	9.0	70000 (4.9)	Golconda	IL	Oct. 1910
17	SW 2-1	114	14.0	30000 (2.2)	nr. Neosho Falls	KS	Sept. 1926
18	MR 1-3A	30	12.5	7200 (4.1)	Blanchard	IA	July 1898
19	MR 2-22	102	11.9	19900 (2.9)	Warrensburg	IA	Aug. 1919
20	MR 4-3	78	12.3	84000 (1.8)	Greeley	NE	June 1896
21	MR 6-2	96	11.4	16000 (3.3)	Lindsborg	KS	Oct. 1941
22	UMV 3-29	15	12.0	20000 (2.6)	nr. Dumont	IA	June 1951
23	GL 2-29	120	12.4	58000 (2.2)	nr. Merril	WI	July 1912
24	MR 1-23	96	10.8	40000 (2.3)	Nemaha	NE	July 1907
25	MR 2-11	96	11.2	24000 (2.3)	Moran	KS	Sept. 1915
26	MR 3-30	60	9.9	60000 (3.6)	Lebo	KS	Nov. 1928
27	UMV 2-5	12	12.1	20000 (3.9)	nr. Bonapart	IA	June 1905
28	UMV 2-8	66	8.8	27000 (3.2)	Bethany	MO	July 1909
29	UMV 3-20B	186	8.4	80000 (2.2)	Galesburg	IL	Sept. 1941
30	UMV 3-21	42	11.0	12600 (2.4)	Thopson Farm	MO	July 1942
31	GL 2-12	120	8.9	67000 (2.4)	Medford	WI	June 1905
32	UMV 2-14	63	9.6	70000 (1.6)	Washington	IA	June 1930
33	GL 3-11	42	11.0	20000 (3.2)	Libertyville	IL	June 1938
34	MR 1-21A	102	8.6	24300 (2.7)	Warsaw	MO	Aug. 1906
35	MR 3-6	48	8.9	45000 (2.7)	Lockwood	MO	Sept. 1925
36	UMV 2-30	24	11.0	10400 (2.8)	Oxford Junction	IA	June 1944
37	MLV 1-3A	84	8.4	20000 (3.3)	Sikeston	MO	Sept. 1898
38	GL 4-5	66	10.0	15000 (4.3)	Butternut	WI	July 1897
39	MR 6-3	24	10.9	5000 (3.6)	Ballard	MO	June 1943
40	MR 1-16A	120	8.2	45000 (1.7)	El Dorado	KS	June 1905
41	MR 6-1	72	8.9	35000 (2.5)	Clifton Hill	MO	June 1942
42	UMV 2-15	24	9.0	13000 (4.4)	Gorin	MO	June 1933
43	UMV 3-28	30	10.7	10500 (3.8)	Mifflin	WI	July 1950
44	MR 1-28	78	8.1	39000 (2.2)	Topeka	KS	Sept. 1909

Table 1 (continued)

Storm no.	US Army Corps of Engineers	Duration (h)	Max 24 h depth (in)	Areal extent (square miles) (associated average depth (in)	Storm center		
					Town	State	Date
45	MR 3-1A	78	9.0	3900 (3.9)	Medicine Lodge	KS	Sept. 1923
46	MR 3-29	30	10.0	14000 (3.1)	Sharon Springs	KS	May 1938
47	UMV 2-22	30	9.0	23400 (2.8)	Gunder	IA	July 1940
48	UMV 4-11	54	9.2	28500 (2.3)	Galva	IL	Aug. 1924
49	MR 7-9	30	10.0	8300 (4.1)	Jerone	IA	July 1946
50	GL 2-30	54	8.9	5000 (3.4)	Viroqua	WI	July 1917
51	MR 3-11	54	8.9	13300 (2.3)	Chanute	KS	Apr. 1927
52	MR 2-23	66	8.7	58350 (2.6)	Bruning	NE	Sept. 1919
53	MR 4-14A	90	8.5	67000 (2.3)	Hazelton	ND	June 1914
54	MR 4-12	42	8.4	13200 (3.7)	Lincoln	NE	Aug. 1910
55	MR 1-3B	30	8.3	20000 (2.5)	Edgehill	MO	July 1898
56	MR 2-3	18	8.0	6800 (3.9)	Wichita	KS	Sept. 1911
57	UMV 1-4A	54	8.0	32000 (2.1)	Minnesota City	MN	June 1899
58	UMV 2-17	12	8.4	15000 (2.9)	Toledo	IA	Aug. 1929
59	OR 4-22	30	8.0	24100 (3.6)	Charleston	IL	Sept. 1926
60	MR 6-16	36	9.1	5100 (2.2)	nr. Bagnell	MO	Aug. 1944
61	MR 7-16	10	10.0	220 (4.3)	nr. Gering	NE	June 1947
62	UMV 1-14B	126	8.0	5000 (2.9)	Worthington	MN	Aug. 1913
63	UMV 1-6	102	8.0	50000 (3.1)	Elk Point	SD	Sept. 1900
64	UMV 1-7A	78	8.0	15200 (3.2)	La Crosse	WI	Oct. 1900
65	UMV 2-19	3	8.4	570 (2.4)	Plainville	IL	May 1941

properties of Ω which were used for the estimation of the joint probability distribution $f_{\Omega}(\omega)$:

(1) The storm orientation Φ is independent of all other random variables of Ω. Owing to the lack of maximum 24 h storm orientation data is was not possible to estimate $f_{\Phi}(\phi)$, and the application of the method was restricted to the case of circular catchments for which the storm orientation Φ will have no effect and the integration over the parameter Φ need not be considered.

(2) The storm elongation parameter C is independent of all other random variables of the vector Ω and follows a distribution $f_C(c)$. However, to simplify the estimation of $G(d)$, this parameter was taken to be a constant equal to the mode of its distribution ($c = 2.0$) as it was shown by Wilson and Foufoula-Georgiou (1990) that small variations in this parameter have little effect on the estimation of the exceedance probabilities.

(3) The parameters K^* and N of the spatial spread function of Eq. (10) are dependent upon each other but are independent of all other random variables of Ω. If we let $K' = \ln K^*$, then the pair (K', N) follows a bivariate normal distribution

$$f_{K'N}(k', n) = \frac{1}{2\pi\sigma_{K'}\sigma_N(1-\rho^2)^{\frac{1}{2}}} \cdot \exp\left\{-\frac{1}{2}H(K', N)\right\} \tag{12}$$

where

$$H(K', N) = \frac{1}{1-\rho^2}\left\{\left(\frac{k'-\mu_{K'}}{\sigma_{K'}}\right)^2 - 2\rho\left(\frac{k'-\mu_{K'}}{\sigma_{K'}}\right)\left(\frac{n-\mu_N}{\sigma_N}\right) + \left(\frac{n-\mu_N}{\sigma_N}\right)^2\right\} \tag{13}$$

Empirical frequency distributions of the parameters k' and n have been given by Wilson and Foufoula-Georgiou (1990), together with details of the fitting procedure which produced the following estimates (obtained using variables in FPS units): $\hat{\mu}_{K'} = -5.437, \hat{\sigma}_{K'} = 1.335; \hat{\mu}_N = 0.597, \hat{\sigma}_M = 0.147$; and $\hat{\rho} = \hat{\rho}_{K',N} = -0.917$.

(4) Based on observations related to the spatial distribution of storm centers of extreme midwestern storms, Wilson and Foufoula-Georgiou (1990) hypothesized that the distribution of storm centers (X, Y) conditional on $d_o^* \geq d_{\min}^*$ (where $d_{\min}^* = 20.32$ cm = 8 in) could be approximated by a transformed bivariate normal distribution independent in each direction. However, in our study, to reduce the computation time required by the Monte Carlo procedure, it has been decided to consider as transposition area a sub-area of about 1 000 000 km^2 (as shown in Fig. 1) where the major concentrations of storm occurrences has been observed. For this sub-area it is reasonable to assume a uniform probability distribution for the spatial distribution of storm centers, i.e.

$$f_{XY}(x, y) = \frac{1}{|A_{\text{tr}}|} \cdot I(x, y) \tag{14}$$

where $I(x, y)$ is an indicator function defined over the region A_{tr} as

$$I(x, y) = \begin{cases} 1 & \text{if } (x, y) \in A_{\text{tr}} \\ 0 & \text{otherwise} \end{cases} \tag{15}$$

(5) The frequency distribution of the maximum 24 h storm center depth D_o^* was modeled by a shifted exponential distribution given by

$$f_{D_o^*}(d_o^*) = \frac{1}{\theta}\exp\left\{\frac{-(d_o^* - d_{\min}^*)}{\theta}\right\} \tag{16}$$

with $d_{\min}^* = 20.3$ cm (8 in). The parameter θ was estimated as $\hat{\theta} = 6$ cm (2.38 in).

(6) The number of extreme storm occurrences per year was modeled by a Poisson distribution given by

$$\text{pr}[Z(1) = \nu] = \frac{e^{-\lambda}\lambda^{\nu}}{\nu!}, \qquad \nu = 0, 1, 2, \ldots \tag{17}$$

The parameter λ, which is equal to the mean number of extreme storms per year, was estimated as 1.07 storms per year. In the present study, this estimate of λ was also used as an estimate of λ' (annual rate of flood events) owing to lack of extreme flood data on which a more accurate estimate of λ' could be based.

Table 2
Parameters of the ARNO model

Water balance component	
Surface runoff	
b	Shape parameter of the storage capacity distribution curve
W_m	Average storage capacity of the upper zone over the entire basin (mm)
Drainage	
$D_{\min}$	Drainage value at the threshold value of the moisture content W_d (mm^{-1} h)
$D_{\max}$	Maximum drainage value (mm^{-1} h)
W_d	Threshold value of moisture content used in calculating drainage (mm)
c	Shape coefficient of the drainage curve: $c = 1$ linear; $c = 2$ quadratic
Deep infiltration	
W_i	Threshold value of moisture content used in calculating deep infiltration (mm)
α	Percentage of $(W_0 - W_i)$ used in calculating deep infiltration
Ground water flow	
K	Depletion rate constant of the lower zone (h^{-1})
n	Number of linear reservoirs
Transfer component	
C_0, D_0	Convectivity ($m\,s^{-1}$), and diffusivity ($m^2\,s^{-1}$), respectively, of the parabolic hydrograph for transfer along hillslopes towards the channel network
C_1, D_1	Convectivity ($m\,s^{-1}$), and diffusivity ($m^2\,s^{-1}$), respectively, of the parabolic hydrograph for transfer along the channel network towards the outlet

3.2. *Rainfall–runoff model parameterization and temporal distribution of storm depths*

As previously mentioned, the ARNO model has 14 parameters (see Table 2) forming the random vector

$$\Psi = \{b, W_m, D_{\min}, D_{\max}, W_d, c, W_i, \alpha, K, n, C_0, D_0, C_1, D_1\} \tag{18}$$

To investigate the effect of the initial soil moisture condition W_0 on flood peaks and decide which parameters of Ψ most significantly affect peak runoff, a sensitivity analysis was performed where one parameter was varied at a time in a wide range around a reference set of basin values as shown in Table 3. In this sensitivity analysis, which is basically referred to flood peak events, the effect of the groundwater flow was disregarded. The results indicated that the frequency of peak runoff is mostly affected by the initial soil moisture condition W_0 and average storage capacity W_m (see Figs. 2(a) and 2(b) and not by other parameters such as, for example, the parameters C_1 and D_1 of the transfer function in the channel network towards the outlet (see Figs. 2(c) and 2(d)). Thus Ψ was reduced to only one parameter, W_m. This parameter, expressing the average storage capacity of the basin, relates to physical characteristics of the basin of interest and therefore its value will in most cases be known by calibration of the R–R model. In such a case W_m will be a deterministic variable.

Table 3
Initial moisture condition and parameters of the ARNO model — reference set and values used in the sensitivity analysis

Symbol	Reference value	Units	Sensitivity analysis		
W_0	50.	mm	0.0	100.	200.
b	0.2		0.0	0.5	1.0
W_m	200.	mm	50.	175.	300.
$D_{\min}$	0.02	$\mathrm{mm\,h^{-1}}$	0.0	0.5	1.0
$D_{\max}$	1.0	$\mathrm{mm\,h^{-1}}$	0.0	2.5	5.0
W_d	100.	mm	0.0	90.	180.
c	2.0		–	–	–
W_t	0.0	mm	50.0	100.	150.
α	0.001		0.0	0.005	0.01
K	0.0	$\mathrm{h^{-1}}$	–	–	–
n	0		–	–	–
C_0	0.5	$\mathrm{m\,s^{-1}}$	0.3	1.15	2.00
D_0	500.	$\mathrm{m^2\,s^{-1}}$	100.	550.	1000.
C_1	2.0	$\mathrm{m\,s^{-1}}$	0.5	2.25	3.0
D_1	5000.	$\mathrm{m^2\,s^{-1}}$	1000.	10000.	20000.

Regarding the parameterization of the temporal distribution of storm depths, we have used the results of Huff (1967), who has performed an extensive frequency analysis of temporal distributions of midwestern storms. He has classified time distribution patterns in four probability groups, from the most severe (first quartile) to the least severe (fourth quartile). The probabilities of each quartile are 0.30, 0.36, 0.19, and 0.15, respectively. For each quartile he has provided a range of mass curves each with its associated probability of exceedance (see Fig. 3, for an example). This statistical description has been used herein to compute the probability density function (pdf) of $T(t)$.

4. Results of simulation and sensitivity analysis

The integrals in Eqs. (3) and (8), needed for the estimation of the exceedance probabilities of extreme precipitation depths and flood peaks, respectively, have been evaluated numerically via a Monte Carlo simulation. Synthetic storms were generated with elliptical shape of major to minor axis equal to two, storm center depth equal to d_0^* (randomly selected from the pdf $f_{D_0^*}(d_0^*)$) and spatial distribution of depths described by the spread function of Eq. (10) with parameters (k', n) (sampled from $F_{K'N}(k', n)$). The triplet (d_o^*, k', n) completely defines the areal extent of the storm A_s (defined here as the area enclosed within the contour depth of 3 in (i.e. 7.62 cm)). Under the assumption of uniform distribution of storm centers within the transposition area A_{tr}, each storm can occur at any position within A_{tr} with the same probability. As only positions which will produce non-zero rainfall and runoff over the basin are of interest, the storms have been transported only within

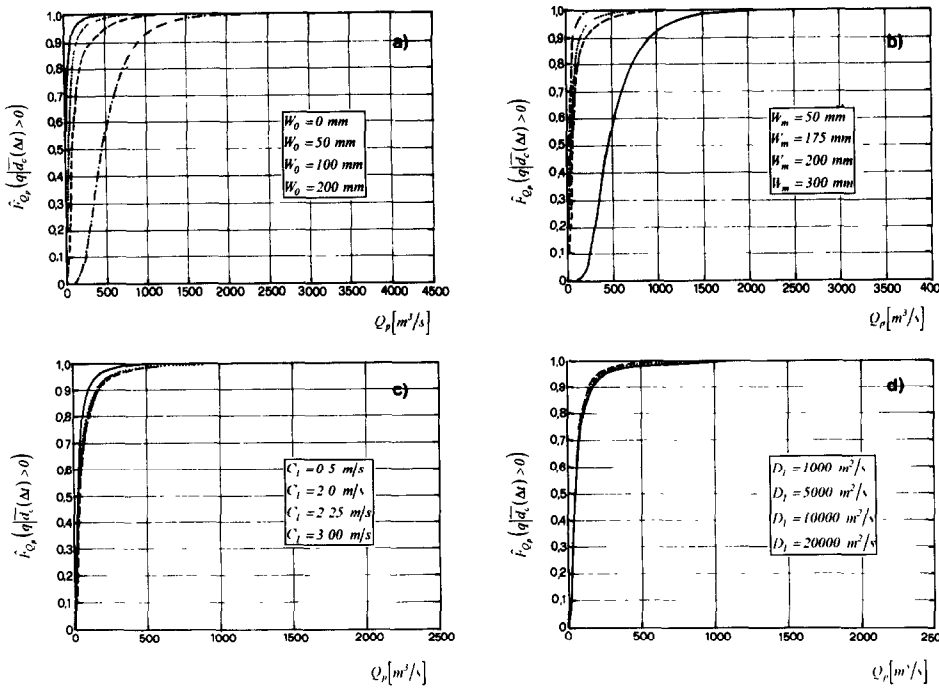

Fig. 2. Frequency curves of flood peaks conditioned on greater than zero average catchment rainfall depth. Sensitivity of frequency curve to (a) initial moisture conditions W_0 (lower curve is for 200 mm and upper curve for 0 mm), (b) average soil storage capacity W_m (lower curve is for 50 mm and upper curve for 300 mm), (c) convectivity coefficient C_1 (upper curve is for 0.50 m s^{-1}), and (d) diffusivity coefficient D_1 (lower curve is for 1000 m^2 s^{-1}) of the transfer function in the channel network towards the basin outlet.

the effective area of the catchment. The effective area (A_{eff}) is defined as the area within which if a storm is centered it will have at least one point common with the catchment and thus will produce non-zero average rainfall depth and runoff. In general, the geometrical shape of A_{eff} cannot be easily described analytically. Instead, it must be determined numerically, except for special cases, as, for example, a circular storm (of radius r_s) and circular catchment (of radius r_c) where A_{eff} is also circular (with radius $r_c + r_s$). It should be noted that A_{eff} changes every time a new storm is transposed over the catchment of interest. To reduce the computations, our analysis has considered a circular basin (of area A_c equal to 200 km^2) and elliptical storms of major axis r_1 and minor axis r_2, and the assumption has been made that the effective area is also elliptical with major axis $(r_c + r_1)$ and minor axis $(r_c + r_2)$.

Following the assumption of uniform distribution of storm centers within A_{tr}, the storm centers also have a uniform distribution within A_{eff}. That is, the probability of the storm center of storm i occurring at any point within its effective area A_{eff_i} is constant and equal to $A_{\text{eff}_i}/A_{\text{tr}}$. Based on this, the probability of obtaining a zero average depth (and thus peak runoff) over the catchment has been approximated

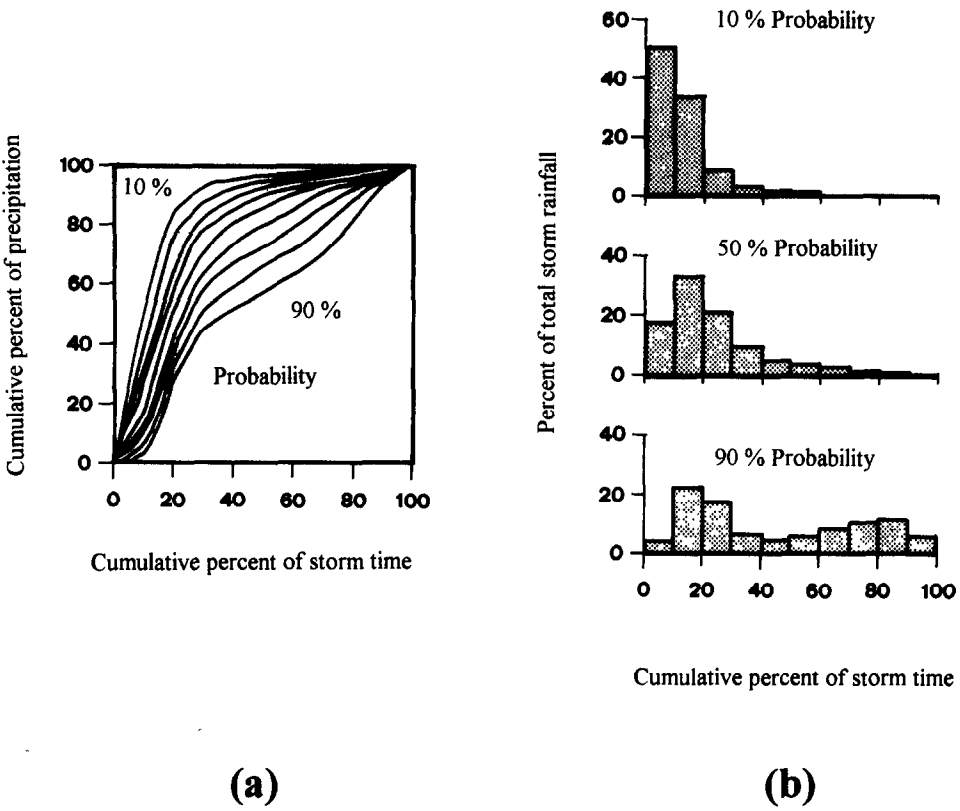

Fig. 3. (a) Time distribution of first quartile storms. The probability shown is the chance that the observed storm pattern will lie to the left of the curve. (b) Selected histograms for first quartile storms (after Huff, 1967).

using the mean effective area as

$$\hat{p}[\overline{d_c}(\Delta t) = 0] = 1 - \overline{A_{\text{eff}}}/A_{\text{tr}} \tag{19}$$

and an estimate of $F(d)$ has been obtained as

$$\hat{F}(d) = [1 - \overline{A_{\text{eff}}}/A_{\text{tr}}] + \hat{F}(d\,|\,\overline{d_c}(\Delta t) \geq 0)[\overline{A_{\text{eff}}}/A_{\text{tr}}] \tag{20}$$

Thus,

$$\hat{G}(d) = [1 - F(d\,|\,\overline{d_c}(\Delta t) \geq 0)][\overline{A_{\text{eff}}}/A_{\text{tr}}] \tag{21}$$

and the annual exceedance probability is estimated as

$$\hat{G}^a(d) = 1 - \exp[-\lambda \hat{G}(d)] \tag{22}$$

It is recalled that the SST method produces values of cumulative rainfall depths averaged over the catchment of interest and estimates of their annual exceedance probabilities. To convert these cumulative depths to flood peaks a disaggregation

scheme is needed to obtain the storm hyetograph, e.g. a sequence of hourly rainfall depths, which can be run through an R–R model to produce runoff hydrographs. A probabilistic disaggregation scheme has been used based on Huff's curves (Huff, 1967), i.e. the temporal distribution of cumulative depths has been randomized according to its probability distribution $F_{T(t)}(\tau(t))$ as discussed above and integration over $F_{T(t)}(\tau(t))$ has been performed. For the estimation of exceedance probabilities of runoff peaks numerical integration over the pdf of the random variables W_0 and W_m is also needed. Determination of $f_{W_0}(w_0)$ requires availability of initial moisture condition data from a large set of extreme storms. Such data were not available in this study and therefore no attempt was made to characterize the pdf of W_0. Instead, several values of W_0 were selected corresponding to a range of initial moisture conditions from totally dry to saturated ($W_0 = 0, 40, 100, 160, 180$, and 200 mm) and evaluation of flood peaks and their exceedance probabilities was performed conditional on these constant W_0 values. If probabilities could be assigned to these values it would be possible to integrate numerically and obtain the unconditional flood peak exceedance probabilities. Similarly, owing to difficulties in estimating the pdf of the parameter W_m (which, in fact, in most cases might be desired to be kept constant to the deterministically obtained value via calibration) no integration over the pdf of W_m has been performed. Instead, a constant value of W_m equal to 200 mm has been considered as a reference value and the frequency analysis has been performed conditional on this value. Other values of W_m can be considered as necessary.

Numerical evaluation (via Monte Carlo simulation) of the stochastic integrals in Eqs. (3) and (8) produced the annual exceedance probability curves of 24 h areally averaged catchment depths $\overline{d_c}$ (Fig. 4(c)) and flood peaks Q_p (parts (a) of Figs. 4–8 for five different initial moisture conditions). In addition, another type of simulation was performed. Fixing W_0 and W_m to a predefined set of values, a given 24 h average catchment depth $\overline{d_c}$ has produced a range of possible flood peak values Q_p, each corresponding to a different disaggregation and having a different chance of occurrence. Let us denote by $\langle Q_p \rangle = E[Q_p|\overline{d_c}]$ the expected value of these Q_p values conditional on a specific constant value of $\overline{d_c}$, where expectation is taken only with respect to the probability distribution of temporal distributions $F_{T(t)}((\tau(t))$ of the cumulative depth $\overline{d_c}$. This expected value of $\langle Q_p \rangle$ and the maximum and minimum possible Q_p values ($Q_{p,\max}$ and $Q_{p,\min}$, respectively) have been computed and have been plotted in parts (b) of Figs. 4–8 for W_0 of 0 mm, 40 mm, 100 mm, 160 mm, and 200 mm, respectively, and W_m of 200 mm. These figures provide an interesting link between the annual exceedance probability curve of 24 h average catchment depths (Fig. 4(c)) and peak flows (parts (a) of Figs. 4–8).

To illustrate the use of these curves, let us consider, for example, Fig. 8 (very wet initial moisture conditions) and select a particular $\overline{d_c}$ depth equal to 300 mm. This depth has a probability of exceedance of approximately 6.6×10^{-4} (see Fig. 4(c)) and can produce Q_p values ranging between 1100 and 3600 $m^3\ s^{-1}$ with an average value of 1600 $m^3\ s^{-1}$ (averaging taken by integrating over the pdf of temporal distributions) (see Fig. 8(b)). The annual probability of exceedance of this average $\langle Q_p \rangle$ value is approximately 1.8×10^{-3} whereas that of $Q_{p,\max}$ is approximately 2.4×10^{-5} and that of $Q_{p,\min}$ is approximately 7.4×10^{-3}. Now we select a particular Q_p value,

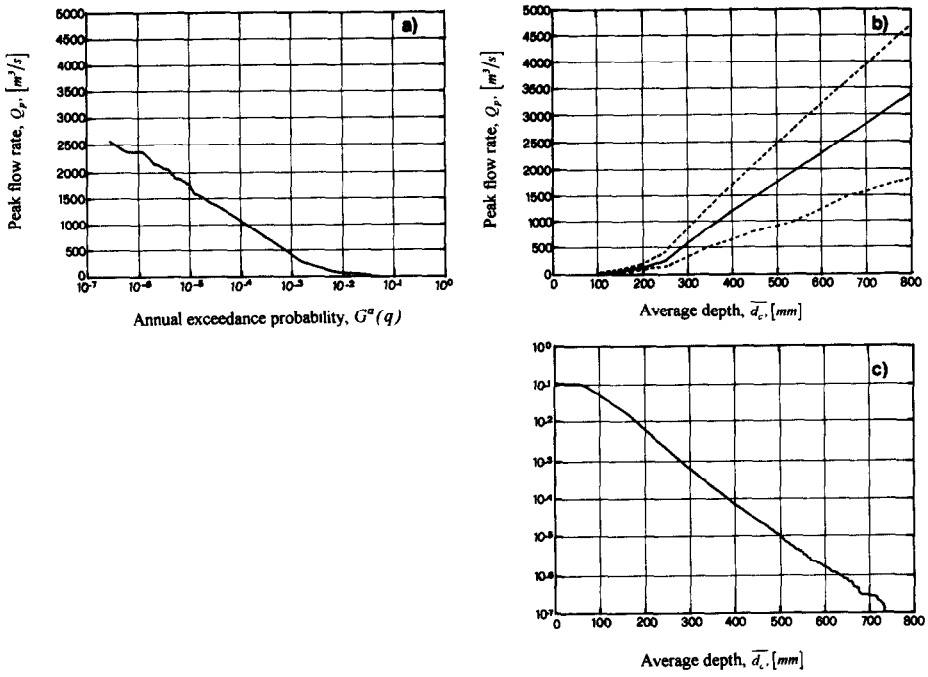

Fig. 4. (a) Annual exceedance probability of flood peak Q_p; (b) flood peak values vs 24 h average catchment depth; (c) annual exceedance probability of the 24 h average catchment rainfall depth d_c. The middle curve in part (b) indicates the values of $E[Q_p|\overline{d_c}]$, where expectation is taken over the pdf of storm depth temporal distributions. The curve $E[\overline{d_c}|Q_p]$ is not shown as it almost coincides with the curve $E[Q_p|\overline{d_c}]$. The upper and lower curves in (b) indicate respectively the maximum and minimum Q_p values that can be obtained from different disaggregations of the same 24 h storm depth. The parameters used are $W_0 = 0$ mm (totally dry) and $W_m = 200$ mm.

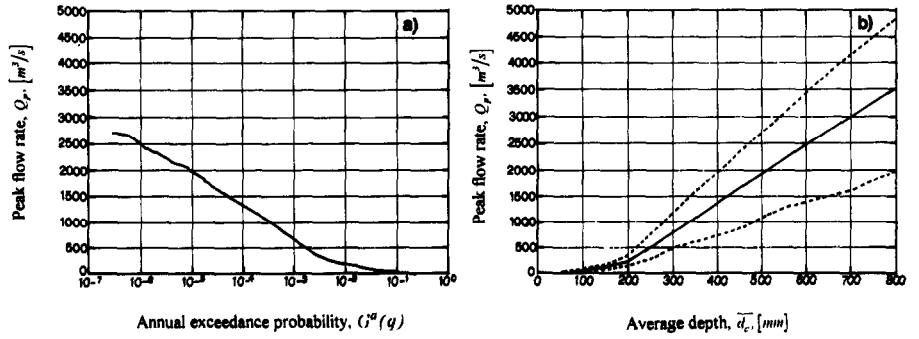

Fig. 5. Same as Fig. 4 but with $W_0 = 40$ mm (dry) and $W_m = 200$ mm. Part (c) is the same as in Fig. 4, and is not repeated.

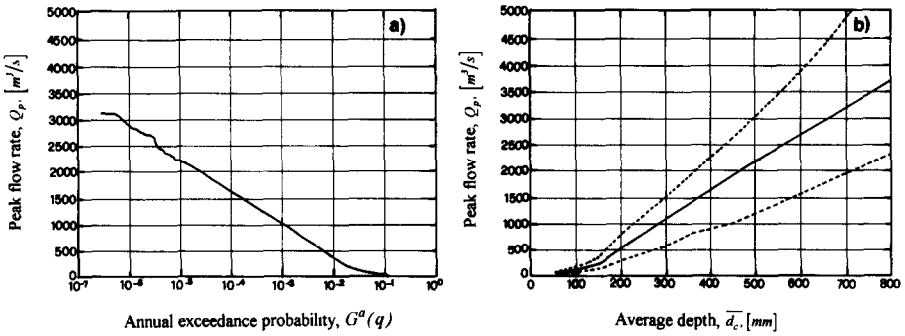

Fig. 6. Same as Fig. 4 but with $W_0 = 100$ mm (medium) and $W_m = 200$ mm. Part (c) is the same as in Fig. 4, and is not repeated.

e.g. 2000 $m^3 s^{-1}$ on the same graph. Its probability of exceedance is approximately 6.9×10^{-4} (see Fig. 8(a)). It should be noted that this Q_p value can be produced by a 24 h average catchment depth ranging between 170 and 550 mm (see Fig. 8(b)) according to chances specified by the pdf of temporal distributions used to disaggregate these 24 h depths to hourly data. The expected value (where again expectation is taken over the pdf of storm depth temporal distributions) of these possible rainfall depths given the specified value of $Q_p = 2000$ m^3 s^{-1}, $\langle \overline{d_c} \rangle = E[\overline{d_c}|Q_p]$, is approximately 380 mm (in our case the curves $E[\overline{d_c}|Q_p]$ and $E[Q_p|\overline{d_c}]$ almost coincide), which has an annual exceedance probability of approximately 1.2×10^{-4}. However, the minimum $\overline{d_c}$ that can produce peak flow of 2000 m^3 s^{-1} has a probability of exceedance approximately equal to 1.4×10^{-2} and a maximum value equal to 3.9×10^{-6}.

Fig. 9 compares the flood peak annual exceedance probability curves for different levels of initial moisture conditions. If one has information about the relative frequency of each initial moisture condition state, e.g. p_i, a weighted average flood peak annual exceedance probability curve could be obtained. That curve would essentially represent the annual frequency estimates obtained by integration over the pdf of $W_0, f_{W_0}(w_0)$. At the same time, the weighted average peak flow rate corresponding

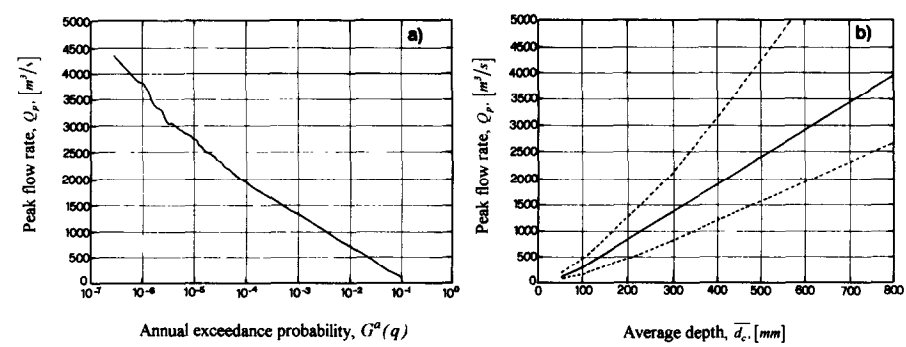

Fig. 7. Same as Fig. 4 but with $W_0 = 160$ mm (wet) and $W_m = 200$ mm. Part (c) is the same as in Fig. 4 and is not repeated.

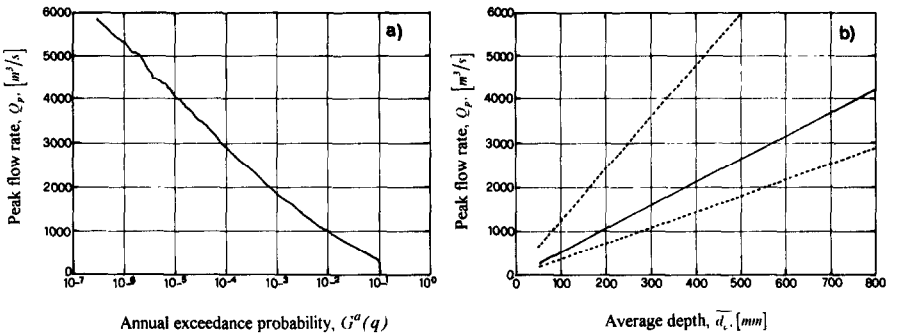

Fig. 8. Same as Fig. 4 but with $W_0 = 200$ mm (saturated) and $W_m = 200$ mm. Part (c) is the same as in Fig. 4, and is not repeated.

to a fixed desired annual exceedance probability could be obtained. For example, given a particular value of the annual exceedance probability the peak flow rate could be obtained as $\Sigma p_i Q_p^i$, where Q_p^i is the peak flow value for initial moisture condition W_0^i, to account for the probabilistic nature of the initial moisture conditions at the beginning of the storm.

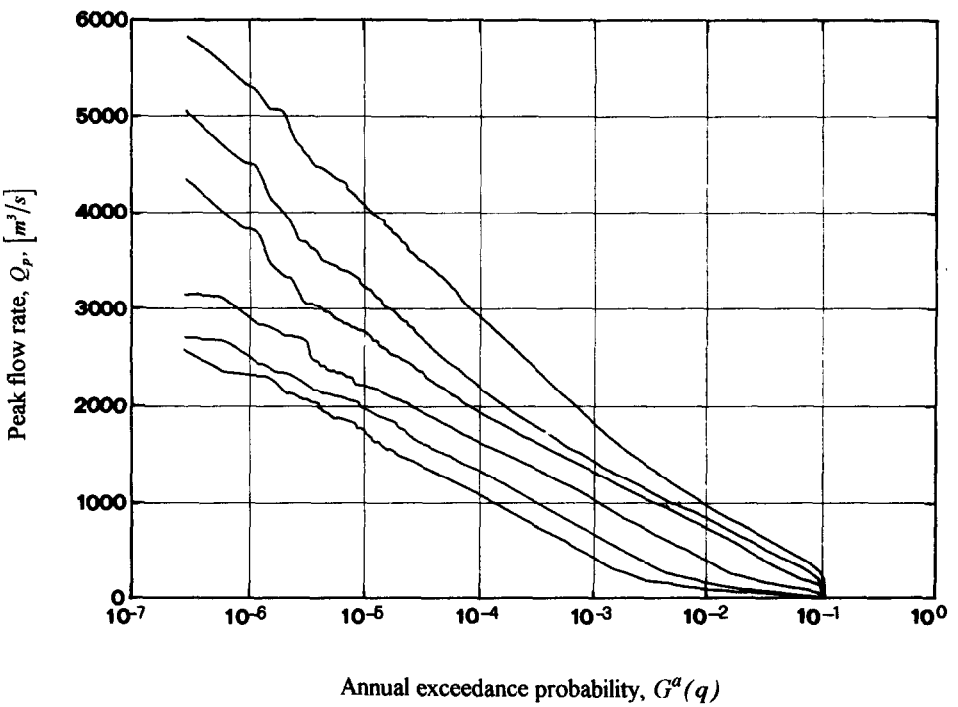

Fig. 9. Comparison of annual exceedance probability curves of flood peaks for different initial moisture conditions ranging from totally dry ($W_0 = 0$ mm) lower curve to saturated ($W_0 = 200$ mm) upper curve. The four middle curves (from bottom to top) are for $W_0 = 40, 100, 160$, and 180 mm, respectively.

Table 4
Effect of initial moisture conditions on frequency of a flood peak of a given magnitude and corresponding magnitudes and frequencies of 24 h relevant average catchment depths

W_0 (mm)	0	40	100	160	180	200
Q_p ($m^3 s^{-1}$)	2000	2000	2000	2000	2000	2000
$G^a(q)$	4.1×10^{-6}	8.9×10^{-6}	2.5×10^{-5}	8.2×10^{-5}	1.71×10^{-4}	6.9×10^{-4}
$\langle \overline{d_c} \rangle = E(\overline{d_c}\|Q_p)$ (mm)	570	530	480	440	420	410
$\overline{d_{c,\min}}$ (mm)	440	410	360	280	240	170
$\overline{d_{c,\max}}$ (mm)	870	810	710	610	580	550
$G^a(\langle \overline{d_c} \rangle)$	2.7×10^{-6}	4.9×10^{-6}	1.45×10^{-5}	3.5×10^{-5}	4.4×10^{-5}	6.2×10^{-5}

To illustrate further the effect of antecedent moisture conditions on design decisions, let us consider as an example the case of an existing hydraulic structure designed to withstand a flood peak of 2000 $m^3 s^{-1}$. The question arises as to what level of flood protection this design event offers. As Table 4 (and Fig. 9) illustrates, depending on the initial moisture condition W_0, the annual exceedance probability $G^a(q)$ of this event varies considerably between approximately 4.1×10^{-6} (totally dry) and 6.9×10^{-4} (saturated) indicating a different level of flood protection in each case. This flood peak value might have been produced by a wide range of 24 h average catchment depths depending on the initial moisture condition W_0 and the temporal distribution of storms as indicated in Table 4. The storm depth expected value (expectation taken with respect to the pdf of temporal distributions only) varies between 870 mm (totally dry) and 550 mm (saturated) and has corresponding annual exceedance probabilities 3.8×10^{-6} to 1.1×10^{-4}. A similar example, where now the probability of exceedance of the design event is fixed and the question arises as to what flood magnitude to use in sizing the hydraulic structure, can be seen in Table 5. As it is observed, the magnitude of that design event varies between 1080 $m^3 s^{-1}$ (totally dry) and 2900 $m^3 s^{-1}$ (saturated) and the expected values of the 24 h average catchment depths corresponding to that design flood vary between 390 mm and 550 mm with corresponding annual exceedance probabilities from 9.8×10^{-5} (totally dry) to 3.8×10^{-6} (saturated). These differences in the exceedance probabilities of storm depths and corresponding flood peaks are reasonable, as it is expected that rare storms coupled with a deterministically fixed always very wet initial moisture condition will produce floods which, by comparison with the frequency of the extreme storm, are not so unusual. These results would change if the probability of finding

Table 5
Effect of initial moisture conditions on magnitude of design floods of a given return period and corresponding magnitudes and frequencies of 24 h relevant average catchment depths

W_0 (mm)	0	40	100	160	180	200
$G^a(q)$	10^{-4}	10^{-4}	10^{-4}	10^{-4}	10^{-4}	10^{-4}
Q_p ($m^3 s^{-1}$)	1080	1320	1620	1940	2180	2900
$\langle \overline{d_c} \rangle = E(\overline{d_c}\|Q_p)$ (mm)	400	410	410	420	460	590
$\overline{d_{c,\min}}$ (mm)	330	320	310	280	250	240
$\overline{d_{c,\max}}$ (mm)	560	580	610	590	630	800
$G^a(\langle \overline{d_c} \rangle)$	7.1×10^{-5}	6.2×10^{-5}	6.2×10^{-5}	4.4×10^{-5}	2.1×10^{-5}	2.0×10^{-6}

the basin so wet before extreme storms was accounted for in the estimation. For that, knowledge of the pdf of W_0 is needed.

In general terms, the results in Figs. 4–8 show that the expected flood peak value $E[Q_p|\overline{d_c}]$ is positioned symmetrically within the band of possible Q_p values produced by a single average depth $\overline{d_c}$, only for the cases with initial moisture conditions W_0 which are either very dry or medium ($W_0 = 0, 40$, and 100 mm). For wetter initial moisture conditions ($W_0 = 160, 180$, and 200 mm) the position of the $E[Q_p|\overline{d_c}]$ curve tends towards the lower Q_p curve while at the same time the width of the possible Q_p values increases (this implies that the range of possible $\overline{d_c}$ values that can produce the same single value of Q_p tends to increase). These aspects affect the slope of the exceedance probability curves of Q_p. In fact, whereas for the first three cases of W_0(0, 40, and 100 mm) the slope in the semi-log frequency plot is almost linear (see parts (a) of Figs. 4–6), when W_0 assumes larger values (160, 180, and 200 mm) an upwards increasing concave shape is observed (see Figs. 7(a)–8(a)). From a probabilistic point of view this means that the exceedance probability of Q_p tends to be larger than the exceedance probability of the relevant average depth as the initial moisture condition tends to increase, i.e. as the soil storage reduces its dumping effect the range of possible average depths that can produce equal values of Q_p (depending on the different temporal distributions) tends to increase, particularly towards average depths with higher exceedance probability. Consequently, as already observed, the exceedance probability of the most extreme flood peaks decreases more slowly than that of the most extreme average depths.

It is worth mentioning that the presented results are affected in their absolute values by the particular set of chosen parameters both for the stochastic structure of storms (vector Ω) and the R–R model (vector Ψ). However, the relative behavior of the exceedance probability curves is expected to remain the same when different sets of parameters are used. Also, the obtained frequency curves are considered reliable between the range of annual exceedance frequencies of approximately 10^{-2} and 10^{-5}. The upper value (10^{-2}) is imposed by the fact that only extreme storms (a 'censored' sample) were used for the estimation of storm characteristics, and the lower value (10^{-5}) is inferred from the fact that up to this range the frequency curves are not affected by the sample size used in the simulation. For example, Fig. 10 compares the frequency curves obtained from a sample size of 400 000 storms (this is the sample size used in all previously reported results) and a much larger sample size of 2 000 000 storms. The curves are almost identical up to annual exceedance probabilities of 10^{-5}.

5. Conclusions

Regional flood frequency analysis has been the subject of considerable research over recent decades (e.g. Stedinger et al., 1993). However, even with regionalization, standard flood frequency analysis methods (based on extrapolation of a hypothesized probability distribution for floods) are not appropriate for estimation of design events of return period greater than 500–1000 years. For very large hydraulic structures and

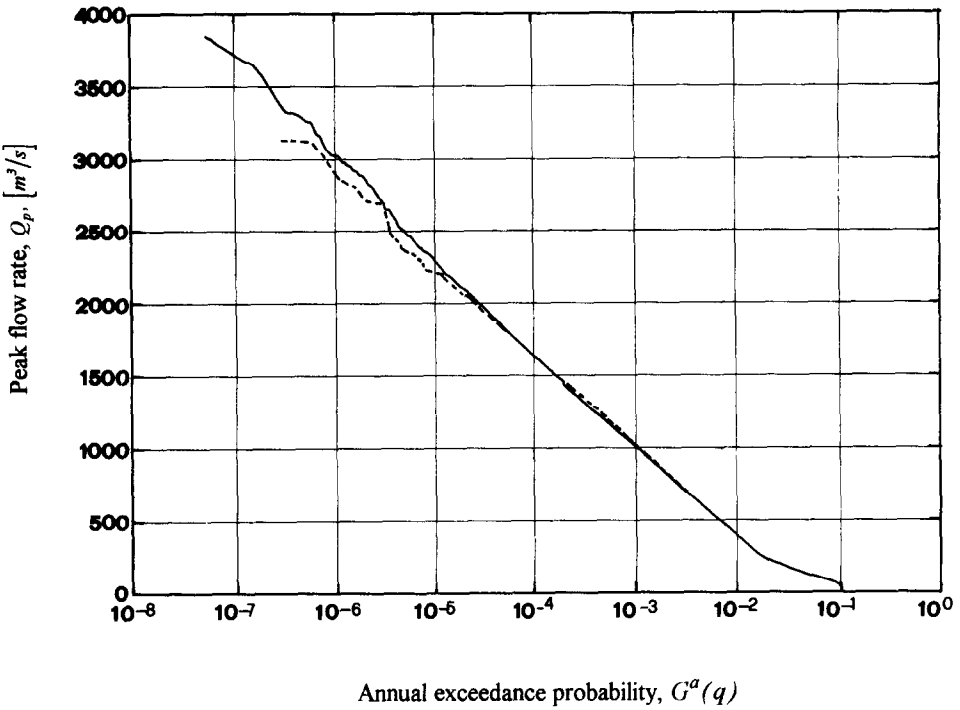

Fig. 10. Comparison of annual exceedance probability curves for sample sizes of 400 000 storms (broken line curve) and 2 000 000 storms (continuous line curve). The parameters used are $W_0 = 100$ mm and $W_m = 200$ mm.

nuclear power plants there is need for design events with annual exceedance probabilities of the order of 10^{-4}–10^{-8} years. Such large design events are usually estimated in a deterministic manner based on the so-called probable maximum flood (PMF) procedure. However, although in concept the PMF values cannot be exceeded, the PMF estimates are random variables that certainly can be exceeded, albeit with a small probability. Not attaching a probability of exceedance to PMF estimates (or other deterministically derived extreme design events) gives a false sense of security or leads to unnecessary overdesign.

Recently, Foufoula-Georgiou (1989) and Wilson and Foufoula-Georgiou (1990) proposed and demonstrated the use of a stochastic storm transposition approach for estimation of the exceedance probability of very extreme precipitation depths over a basin. The results were encouraging in the sense that the method yielded robust estimates of very infrequent precipitation depths. In this paper, the SST approach has been extended to a probabilistic procedure for estimation of annual exceedance probabilities of flood peaks by coupling it with a rainfall–runoff model. In addition, to the stochastic description of storm characteristics and storm positions, the present extension to flood frequency estimation accounts for the probabilistic description of storm temporal distributions, initial moisture conditions, and other parameters of the

rainfall–runoff model that could result in considerably different estimates of flood peaks from the same average catchment depth. The results of our analysis have been reported in such a way as to facilitate an appreciation of the variability of the flood peaks (and their associated exceedance probabilities) that can be produced from a basin for a given specific average catchment depth owing to the variability of the temporal distribution of storm depths and variability in initial soil moisture conditions. The results highlight the importance of the unequal frequency of design storm depths and flood peaks, which is even more pronounced for very wet antecedent moisture conditions.

Although the issue of deterministic vs. risk-based design of very large hydraulic structures is controversial on philosophical and even political grounds, the problems of offering an equal level of flood protection to existing or new sites and making decisions about the need for updating old structures are pragmatic. Even if one has reservations about the absolute value of the obtained frequency estimates, the proposed technique, if used on a comparative basis, offers an objective way of assessing the safety level of existing and new hydraulic structures and of determining the priority for costly retrofitting of old dams according to their comparative level of flood protection.

Acknowledgment

This work was supported in part by NATO Collaborative Research Grant CRG 890434 and NSF Grants CES-8957469 and EAR-9117866.

References

Abbott, M.B., Bathurst, J.C., Cunge, J.A., O'Connell, P.E. and Rasmussen, J., 1986. An introduction to the European Hydrologic System–Système Hydrologique Européen, 'SHE', 1: History and philosophy of a physically-based, distributed modelling system, J. Hydrol., 87(1–2): 45–77.

Huschke, R.E. (Editor), 1959. Glossary of Meteorology. American Meterological Society, Boston, MA.

Foufoula-Georgiou, E., 1989. A probabilistic storm transposition approach for estimating exceedance probabilities of extreme precipitation depths. Water Resour. Res., 25(5): 799–815.

Franchini, M. and Pacciani, M., 1991. Comparative analysis of several conceptual rainfall–runoff models. J. Hydrol., 122: 161–219.

Kraeger, B.A. and Franz, D.D., 1992. Determining the frequency of extreme flood events. Hydro Rev., XI(4): 60–67.

Huff, F.A., 1967. Time distribution of rainfall in heavy storms. Water Resour. Res., 3(4): 1007–1019.

Stedinger, J.R., Vogel, R.M. and Fourfoula-Georgiou, E., 1993. Frequency analysis of extreme events. In: Handbook of Hydrology. McGraw–Hill, New York, Chapter 18.

Todini, E., 1996. The ARNO rainfall–runoff model. J. Hydrol., 175: 339–382.

US Army Corps of Engineers, 1945–. Storm rainfall in the United States. Office of the Chief of Engineers, Washington, DC.

Wang, B.-H. and Jawed, K., 1986. Transformation of PMP to PMF: case studies. J. Hydraul. Div. ASCE, 112(7): 547–561.

Wilson, L.L. and Foufoula-Georgiou, E., 1990. Regional rainfall frequency analysis via stochastic storm transposition. J. Hydrol. Eng. ASCE, 116(7): 859–880.

World Meteorological Organization, 1973. Manual for Estimation of Probable Maximum Precipitation. Oper. Hydr. Rep. 1, WMO 332, Geneva.

Yankee Atomic Electric Company (YAEC), 1984. Probability of exceedance of extreme rainfalls and the effect on the Harriman dam. YAEC, Flamingham, MA.